Acta Crystallographica Section D
Biological Crystallography
ISSN 0907-4449

Involvement of the distal Arg residue in Cl^- binding of midge larval haemoglobin

Takao Kuwada,[a]* Tomokazu Hasegawa,[b] Takashi Takagi,[c] Toshiro Sakae,[a,d] Isamu Sato[a,e] and Fumio Shishikura[a,f]

[a]Laboratory for Electron Beam Research and Application (LEBRA), Institute of Quantum Science, Nihon University, Funabashi, Chiba 274-8501, Japan, [b]Rigaku Co., Akishima, Tokyo 196-8666 Japan, [c]Peptide Door Co. Ltd, Takasaki, Gunma 370-0854, Japan, [d]Department of Histology, Cytology and Development Anatomy, School of Dentistry at Mastudo, Nihon University, Mastudo, Chiba 274-8587, Japan, [e]Advanced Research Institute for the Science and Humanities, Nihon University, Chiyoda-ku, Tokyo 102-8251, Japan, and [f]Division of Chemistry, Department of Liberal Education, Nihon University School of Medicine, Itabashi-ku, Tokyo 173-8610, Japan

Correspondence e-mail: kuwadat@lebra.nihon-u.ac.jp

Received 15 December 2010
Accepted 23 March 2011

PDB References:
haemoglobin component V, 500 m*M* NaCl at pH 4.6, 3arj; 1 *M* NaCl at pH 4.6, 3ark; 500 m*M* NaCl at pH 5.5, 3arl.

Monomeric haemoglobin component V (Hb V) from the larva of the midge *Propsilocerus akamusi* shows high Cl^- affinity under high salt concentrations at acidic pH. In order to understand the structural changes that depend on Cl^- binding, crystal structures of Hb V were determined under acidic high-salt conditions and the structural changes arising from different haem-bound ligands were simulated. Crystal structures of Hb V under acidic high-salt conditions indicated that the side chain of ArgE10 on the distal face of the haem contributes to stabilizing haem-bound Cl^-. The conformation of the Arg side chain in the Cl^--bound form was almost identical to that in ligated Hb V at neutral pH but not to that in met Hb V under acidic salt-free conditions. Furthermore, preliminary molecular-dynamics simulations also indicated that the swinging of the Arg side chain into the haem pocket depends on Cl^- ligation. This result suggests that, like pH change, Cl^- binding affects the location of the distal Arg residue. Owing to the increased positive electrostatic potential observed in the haem pocket at acidic pH, it was concluded that electrostatic changes caused by pH change and anionic ligand binding may affect the behaviour of the polar Arg residue.

1. Introduction

The fourth-instar larva of the midge *Propsilocerus akamusi* (Diptera: Chironomidae) has at least 11 haemoglobin (Hb) components that have been classified into two distinct types, low absorbance (L-type) and normal absorbance (N-type), on the basis of their spectroscopic properties (Fukuda *et al.*, 1993). One of the most remarkable characteristics of Hb component V (Hb V), which is representative of L-type Hb, is the replacement of the His residue at the E7 helical position by a nonpolar Ile residue. In general, the HisE7 residue on the distal side of the haem acts as a proton donor in a hydrogen bond that stabilizes the haem-bound ligand molecule and is conserved in many globin proteins (Phillips, 1980; Phillips & Schoenborn, 1981; Shaanan, 1983; Olson *et al.*, 1988). However, an Arg residue at the E10 helical position has been indicated to maintain the ligand-binding properties of Hb V (Koshikawa *et al.*, 1998; Yamamoto *et al.*, 2003; Kuwada *et al.*, 2010). A contribution of ArgE10 to ligand binding has also been observed in myoglobin (Mb) from the mollusc *Aplysia limacina*, in which position E7 is occupied by a Val residue (Bolognesi *et al.*, 1990; Mattevi *et al.*, 1991; Conti *et al.*, 1993). It is of note that although ArgE10 is considered to have been selected independently as a functional substitute for the

nonpolar E7 residue during molecular evolution in each globin lineage, the characteristic swinging movement of the ArgE10 side chain plays an important role in the regulation of functional properties in both *P. akamusi* Hb V and *A. limacina* Mb (Conti *et al.*, 1993; Kuwada *et al.*, 2010).

Crystal structures of Hb V under different pH conditions indicated pH-dependent structural changes, including movement of ArgE10 (Kuwada *et al.*, 2010). Although at neutral pH the ArgE10 side chain lies above the distal haem face and contributes to stabilizing the haem-bound ligand molecule (swung-in form), a change to acidic or alkaline pH results in a swinging movement of the Arg side chain outwards from the haem pocket (swung-out form); direct contacts between ArgE10 and the ligand molecule could not be observed under these conditions. A similar ligand-binding-dependent conformational change of the ArgE10 side chain was observed in *A. limacina* Mb, suggesting that the behaviour of the Arg side chain is key to controlling the functional properties of these globin molecules (Conti *et al.*, 1993; Kuwada *et al.*, 2010). In Hb V, a pH-dependent partial shift of the F-helix C-terminus, which includes the proximal His residue (HisF8), was observed in addition to the movement of ArgE10. Because the coupled movement of distal and proximal sides of the haem at each pH condition can affect the haem environment, the movement of the haem region was thought to contribute to tuning the pH-dependent functional properties observed in this insect Hb: acidic and alkaline Bohr effects and a unique autoxidation reaction of oxy Hb V (Koshikawa *et al.*, 1998; Kamimura *et al.*, 2003; Yamamoto *et al.*, 2003).

In contrast, paramagnetic proton nuclear magnetic resonance (H-NMR) studies clarified the characteristic anion affinities in methaemoglobin (met Hb) V under acidic and alkaline conditions: Cl^- affinity under high salt (NaCl) concentrations at acidic pH and OH^- affinity at alkaline pH (Koshikawa *et al.*, 1998; Yamamoto *et al.*, 2003). Both H-NMR studies indicated pH-dependence of the anion affinities and a contribution of ArgE10 to anion binding. However, previous crystallographic studies were unable to confirm the contribution of ArgE10 to binding these anions because the Arg side chain adopts a swung-out conformation at acidic and alkaline pH (Kuwada *et al.*, 2007, 2010). The disagreement between H-NMR and crystallographic studies regarding the contribution of Arg to ligand binding suggests that various conditions can affect the conformation of the ArgE10 side chain and moreover the structure of the haem region in Hb V. In fact, anionic ligand binding to the haem iron has been shown to bring ArgE10 into the swung-in conformation in *A. limacina* Mb (Bolognesi *et al.*, 1990; Mattevi *et al.*, 1991; Conti *et al.*, 1993). However, the mechanism of anion-binding-induced and pH-induced Arg movements in these invertebrate globin molecules has not been clarified.

The binding of Cl^- to the haem iron is a unique characteristic of Hb V that has not been reported in other globin proteins (Yamamoto *et al.*, 2003); therefore, it can be expected that analysis of the Cl^--bound form of Hb V might reveal new information about the diversification of structural and functional mechanisms in globin proteins. In this study, we determined crystal structures of Hb V under high salt concentration (500 m*M* and 1 *M* NaCl) at acidic pH (pH 4.6 and 5.5) in order to examine the characteristics of Cl^- binding and high-salt-dependent structural changes in the haem region. Comparison of the present structural data with data from previous work, in which Hb V structures were determined under various pH conditions without salt (Kuwada *et al.*, 2010), allowed the effects of high salt concentrations on the Hb V structure to be detected independently from the effects of pH. Moreover, preliminary molecular-dynamics-based simulations were also performed in order to better understand the characteristic swinging movement of the ArgE10 side chain. On the basis of these results, we describe possible mechanisms underlying the swinging movement of the Arg side chain and its dependence on changes in the electrostatic environment.

2. Materials and methods

2.1. Crystallization and X-ray diffraction analyses

We purified Hb V from fourth-instar larvae of the midge *P. akamusi*, as described by Fukuda *et al.* (1993). The Hb solution was replaced by 50 m*M* Tris–HCl pH 7.0. Crystallization was carried out using hanging-drop vapour-diffusion techniques at 293 K in air. We prepared the following reservoir solutions: 15–17.5% PEG 3350, 500 m*M* or 1 *M* NaCl, 0.1 *M* sodium acetate pH 4.6 and 15–17.5% PEG 3350, 500 m*M* NaCl, 0.1 *M* Bis-Tris pH 5.5. The crystals were grown in a drop consisting of the protein solution (approximately 10 mg ml^{-1}) mixed with an equal amount of each reservoir solution. The crystals appeared within 5 d regardless of the crystallization conditions.

Surplus Hb V crystals grown in 500 m*M* NaCl at pH 4.6, which were not suitable for use in X-ray diffraction analyses, were dissolved in 5 µl 500 m*M* NaCl, 0.1 *M* sodium acetate pH 4.6 and used for spectroscopic analysis of the ligand state according to Kuwada *et al.* (2010). The absorption spectra of solutions containing dissolved crystals were measured in the UV–Vis region using a NanoDrop ND-1000 spectrophotometer.

X-ray diffraction data were collected from each crystal using Cu $K\alpha$ wavelength X-rays from a rotating-anode X-ray generator (Rigaku ultraX 18) and an imaging-plate detector (Rigaku R-AXIS IV^{++}). Crystals were flash-cooled at 100 K in a stream of cold nitrogen without cryoprotectant to prevent crystal cracking. Diffraction data from Hb V crystals were collected to 1.81 Å resolution. The diffraction data sets were processed using *CrystalClear* (Rigaku Co., Tokyo, Japan). The data-collection and processing parameters of the crystals are summarized in Table 1.

2.2. Refinements and structural analysis

The crystal structures of *P. akamusi* Hb V in each high-salt condition were solved at 3.5 Å resolution by the molecular-replacement (MR) method with *CNX* (MSI Inc., California, USA). The search model used was the previously determined structure of Hb V (PDB entry 1x3k; Kuwada *et al.*, 2007)

Table 1
Data-collection and refinement statistics.

Values in parentheses are for the highest resolution shell.

	500 m*M* NaCl pH 4.6	1 *M* NaCl pH 4.6	500 m*M* NaCl pH 5.5
Diffraction data			
Space group	$P2_12_12$	$P2_12_12$	$P2_12_12$
Unit-cell parameters			
a (Å)	65.31	65.20	65.33
b (Å)	75.06	75.25	75.15
c (Å)	33.47	33.53	33.47
Resolution (Å)	49.27–1.81 (1.87–1.81)	49.28–1.81 (1.87–1.81)	49.30–1.81 (1.87–1.81)
No. of recorded reflections	212742	216321	215993
No. of unique reflections	15605	15655	15614
Completeness (%)	99.8 (100.0)	99.9 (100.0)	99.8 (100.0)
$R_{\rm merge}$†	0.058 (0.164)	0.056 (0.168)	0.048 (0.120)
$\langle I/\sigma(I)\rangle$	26.6 (12.6)	26.0 (12.2)	34.9 (17.2)
Multiplicity	13.63 (13.26)	13.82 (13.70)	13.83 (13.69)
Model statistics			
R factor	0.180	0.187	0.179
$R_{\rm free}$	0.208	0.218	0.205
No. of atoms (ions)			
Protein	1213	1213	1213
Haem	43	43	43
Cl^-	5	5	5
Solvent	296	299	298
R.m.s. deviations			
Bond lengths (Å)	0.01825	0.01923	0.01931
Bond angles (°)	1.53619	1.68635	1.60890
Mean *B* factors (Å^2)			
Main-chain atoms	14.5	13.5	11.6
Side-chain atoms	17.0	17.0	14.8
Haem atoms	18.7	18.4	17.2
Haem-bound Cl^- ion	24.2	21.6	20.7
Cl^- ions in solvent region	21.5	20.3	19.1
Water atoms	30.1	29.7	28.7
Ramachandran plot‡ (%)			
Favoured	99.3	98.7	98.7
Additional allowed	0.7	1.3	1.3

† $R_{\rm merge} = \sum_{hkl}\sum_i |I_i(hkl) - \langle I(hkl)\rangle| / \sum_{hkl}\sum_i I_i(hkl)$. ‡ Stereochemistry was assessed by *MolProbity* (Chen *et al.*, 2010).

edited according to Kuwada *et al.* (2010). The MR models were refined using *CNX* functions while increasing the resolution stepwise to the highest resolution. The missing portions of each Hb V model were manually built using *X-BUILD* (*QUANTA*; MSI Inc.) guided by a composite-annealed OMIT map. The models were fitted to the electron-density map and refined using *CNX* and *REFMAC* (Winn *et al.*, 2001). The haem, Cl^- ions and solvent molecules were added after all of the amino-acid residues had been modelled. The haem was refined by several rounds of manual rebuilding using *X-BUILD* and *REFMAC* restrained refinement. Water molecules were added using *X-SOLVATE* (*QUANTA*; MSI Inc.) guided by $F_o - F_c$ electron-density maps contoured at 3σ and were manually verified in *X-BUILD*. According to Numoto *et al.* (2008), Cl^- ions were added in exceedingly high peaks of electron density found within the solvent region and at the haem-ligand position. The quality of the final models was assessed using *MolProbity* (Chen *et al.*, 2010). Refined statistics for all crystal structures are shown in Table 1.

For comparison of the Hb V structures, the Hb V coordinates were superimposed using 92 C^α atoms of the B, G and H helices according to the BGH frame (Baldwin & Chothia, 1979). Calculations of root-mean-square deviations (r.m.s.d.s) and measurements of the bond distances between atoms were performed using *Swiss-PdbViewer* (Guex & Peitsch, 1997) and *CONTACT* (Collaborative Computational Project, Number 4, 1994), respectively. The hydrogen bonds between the globin chain and each Cl^- ion were estimated using the *PDBeMotif* web interface (Golovin & Henrick, 2008). Electrostatic potential surface maps were generated using the *APBS* tools in *MolFeat* (FiatLux Co., Tokyo, Japan), in which electrostatic calculations at each pH were performed with *PDB2PQR* (Dolinsky *et al.*, 2004) and *APBS* (Baker *et al.*, 2001). Structural figures were drawn using *PyMOL* (DeLano, 2002).

2.3. Molecular-dynamics simulation

Two starting Hb V models were prepared to simulate the structural change of ArgE10 depending on ligand type. The first, the ArgE10 swung-out form in which the Arg side chain swings outwards from the haem pocket, was taken from the Hb V structure under salt-free conditions at pH 4.6 (PDB entry 2zwj; Kuwada *et al.*, 2010), and the other, the Arg swung-in form in which the Arg side chain lies above the distal haem face, was taken from the Hb V structure at 500 m*M* NaCl and pH 4.6 reported in this paper (PDB entry 3arj). For each starting model we ran simulations of two different haem-bound ligands, an anion (Cl^-) and a water molecule. The Fe—Cl^- bond in the Cl^--bound model was restrained to be 2.4 Å in length according to the Hb V structure reported in this paper using a force constant of 0.8 mdyn Å^{-1} (Xiao *et al.*, 2005). The charge on the Cl^- ion was assumed to be −1.0e. The Fe—O (water) bond in the water-bound model was tentatively restrained using the same conditions as the Fe—Cl^- bond as the force constant for the Fe—O bond is uncertain. Glu10, Glu56 and basic amino-acid residues in the Hb V models were protonated according to the pK_a values predicted by *PROPKA* (Li *et al.*, 2005; Bas *et al.*, 2008) to represent pH 4.6.

The molecular-dynamics (MD) simulations were performed using *GROMACS*4.0 (Hess *et al.*, 2008) with the GROMOS96 53a5 force field (Oostenbrink *et al.*, 2004). Each system containing one Hb component, including a haem group and approximately 11 200 molecules of SPC water, was neutralized by replacing water molecules with Na^+ ions. Simulations were carried out at a constant temperature of 293 K within a cubic box using periodic boundary conditions. Long-range electrostatic interactions were treated using the particle mesh Ewald method with a grid spacing of 0.12 nm and a nonbonded pair list cutoff of 0.9 nm, with the pair list updated every five steps. A time step of 2 fs was used in all simulations. After energy minimization using a steepest-decent method, each system was equilibrated for 100 ps in the NVT ensemble and for an additional 100 ps in the NPT ensemble. The *SHAKE* algorithm was used to constrain the length of bonds involving H atoms. Production MD was run for a total simulation time of 25 ns.

3. Results

3.1. Crystal structures of Hb V in the presence of a high salt concentration at acidic pH

In this study, we determined three crystal structures of *P. akamusi* Hb V under conditions of high salt concentration and acidic pH (Table 1). Hb V crystals grown under these conditions belonged to space group $P2_12_12$, with one monomer per asymmetric unit, identical to the previous Hb V crystals grown at acidic pH (Kuwada *et al.*, 2007, 2010). The Hb V models at 500 m*M* NaCl at pH 4.6, 1 *M* NaCl at pH 4.6 and 500 m*M* NaCl at pH 5.5 were refined at 1.81 Å resolution to *R* factors of 0.180 ($R_{\rm free}$ = 0.208), 0.187 ($R_{\rm free}$ = 0.218) and 0.179 ($R_{\rm free}$ = 0.205), respectively. Each refined model consisted of a complete polypeptide chain (152 amino-acid residues), one haem group, approximately 300 water molecules and five Cl^- ions, including one as a haem ligand. The r.m.s.d.s among these Hb V models were less than 0.08 Å for all 152 C^α atoms of the globin chain and less than 0.33 Å for all 1213 atoms of the globin chain, indicating that no remarkable differences were present between the models.

Fig. 1 shows electron-density maps on the distal side of the haem in Hb V under different salt conditions at acidic pH. In aquomet Hb V under salt-free conditions at pH 4.6 (Kuwada *et al.*, 2010) the density of the haem-bound water molecule (visible at 9.8σ in the $F_o - F_c$ map) was almost identical to that of a water molecule, W1, located at the haem-pocket entrance (10.7σ; Fig. 1*a*). In contrast, under high-salt conditions at acidic pH high electron density (15.1–17.7σ) was observed at the haem-ligand position, although the density of W1 (8.9–10.9σ) was similar to that in the salt-free condition (Fig. 1*b*). The optical absorption spectrum of the dissolved Hb V crystal sample displayed a red shift of the Soret band from approximately 400 to 410 nm and increased and decreased absorption spectra at approximately 510 and 640 nm, respectively (Fig. 2); these findings are characteristics of Cl^--bound Hb V (Yamamoto *et al.*, 2003). From these results, we concluded that the haem-ligand positions were occupied by a Cl^- in the Hb V crystals grown under high salt concentration at acidic pH. In all three refined Hb V models the haem-bound Cl^- contacts the haem iron with a distance of approximately 2.4 Å.

3.2. The haem region of Hb V structures under high salt concentration

The overall folds of the Hb V structures under high salt concentration at acidic pH were almost identical to that at acidic pH without salt, with r.m.s.d.s for C^α atoms of less than 0.16 Å for each pair. However, a significant difference was observed in the orientation of the ArgE10 side chain between the high-salt and salt-free conditions at acidic pH. Although the ArgE10 side chain swings out toward the solvent region at acidic pH without salt or in the presence of 200 m*M* ammonium sulfate (Kuwada *et al.*, 2007, 2010; Figs. 1*a* and 3), the Arg side chain lies above the distal haem face at high NaCl concentration (Figs. 1*b* and 3). The N^ε atom and NH of ArgE10 under all three high-salt conditions contact the haem-bound Cl^- with distances of approximately 3.2 and 3.5 Å, respectively, suggesting that the N^ε atom forms a weak hydrogen bond to the Cl^- ion. This Arg conformation was almost identical to that in ligated Hb V at neutral pH without salt (Fig. 3), in which the Arg on the distal haem face also forms hydrogen bonds to the ligand molecule (Kuwada *et al.*, 2010).

Fig. 3 shows the overlap of the haem region under different pH and salt conditions. Structural comparison indicated a slight displacement of the haem towards the proximal side under high salt concentration at acidic pH. The CHA–CHC axis of the haem under these conditions tilts approximately 4° compared with that at acidic pH without salt. Haem displacement was also observed in Hb V at neutral pH (Kuwada *et al.*, 2010; Fig. 3). In contrast, no significant differences were observed on the proximal side of the haem between Hb V structures at different salt concentrations at acidic pH. The C-terminal segment of the F helix, GlyF6–HisF8, was found to become unstable and to be stretched depending on the pH change (Kuwada *et al.*, 2010; Fig. 3). However, the F-helix C-terminus at acidic high-salt conditions displays a 3_{10}-helix or an α-helix almost identical to that at acidic pH without salt.

3.3. MD simulations of the swinging movement of ArgE10

As a supplementary analysis to confirm the swinging movement of the ArgE10 side chain, MD simulations were carried out on four different systems: combinations of two different Arg orientations and two different haem ligands. Fig. 4 shows an example of the time evolution of the distances between the haem ligand and N^ε and NH of the ArgE10 side chain during 25 ns MD simulations for each system. In the simulation starting with the ArgE10 swung-out form binding a Cl^- ion, the Arg side chain swung into the distal haem pocket early and then remained to contact the haem-bound Cl^- during the simulation. At the end of the 25 ns simulation the distances between the Cl^- and the N^ε and NH of ArgE10 were approximately 3.3 and 3.2 Å, respectively, in the case shown in Fig. 4; these distances are similar to those in the crystal structures of Cl^--bound Hb V. Conservation of the contacts between the Cl^- ion and the Arg side chain during the simulation was also observed when the Arg swung-in form binding a Cl^- ion was used as a starting model. In contrast, in the simulation starting with the Arg swung-in form binding a water molecule the Arg side chain swung out from the haem pocket and then moved flexibly in the solvent region for the remainder of the simulation time. Flexible movement of the Arg side chain was also observed in the case using the Arg swung-out form binding a water molecule.

These simulations were run five times each to identify whether the above observations were repeatable. It was found that the conformation of ArgE10 in these simulations did not correspond exactly to that in crystallographic structures of Hb V (Supplementary Fig. 1[1]). However, the ligand-depen-

[1] Supplementary material has been deposited in the IUCr electronic archive (Reference: MH5040). Services for accessing this material are described at the back of the journal.

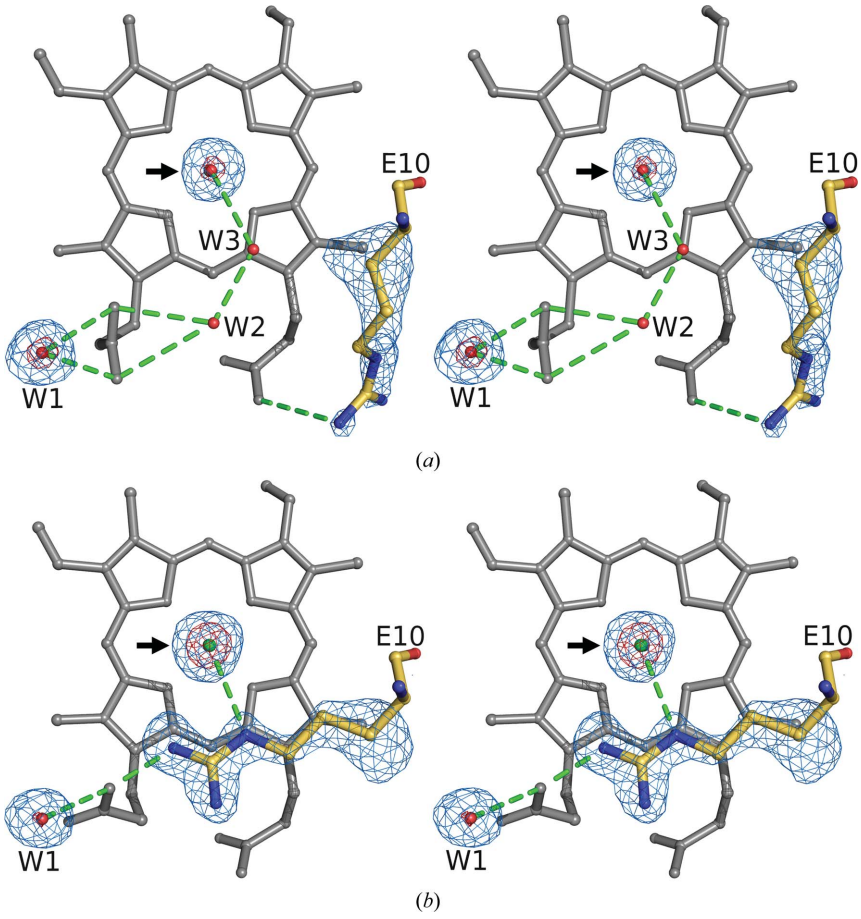

Figure 1
Stereoview of the hydrogen-bond network on the distal side of the haem of Hb V at pH 4.6 under (*a*) salt-free conditions (aquomet Hb V; PDB entry 2zwj) and (*b*) at 500 m*M* NaCl concentration. Light-green broken lines represent the hydrogen bonds between the ArgE10 (E10) side chain, the haem groups and the distal side water molecules (W1–W3). Blue and red nets represent $F_o - F_c$ maps contoured at 2σ and 8σ, respectively, calculated without the haem ligand, a neighbouring water molecule (W1) and the ArgE10 side chain. Arrows indicate electron density for the exogenous ligand. The haem is shown as grey sticks in each figure. For the haem ligand under high-salt conditions, Cl^- is fitted and shown as a green ball.

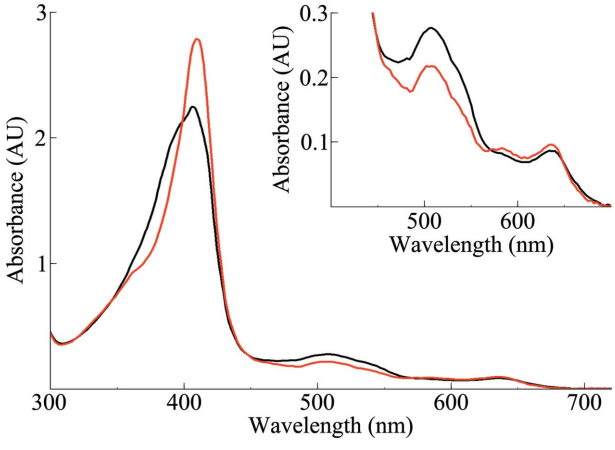

Figure 2
The UV–visible absorption spectra of Hb V under 500 m*M* NaCl (red) and salt-free (black) conditions at pH 4.6. The visible region of the spectrum (400–700 nm) is enlarged in the inset.

dent swinging movement of ArgE10 could be reproducibly observed in the repeated simulations. In addition, although it was probable that the difference between the protonated and deprotonated states of the haem propionate groups also affects the location of the polar Arg side chain, the dependence of the Arg behaviour on different ligands was confirmed in the simulations regardless of the protonation status of the haem propionate groups.

4. Discussion

4.1. Binding of Cl^- and dependent structural changes in *P. akamusi* Hb V

Yamamoto *et al.* (2003) described the characteristic Cl^- binding to haem iron and the contribution of ArgE10 to its stabilization in Hb V under acidic high-salt conditions. In agreement with their results, crystallographic analyses of Hb V indicated the presence of a Cl^- ion at the sixth ligand position of haem iron under acidic high-salt conditions. Met-globins are known to bind a number of different anions, such as N_3^-, CN^-, NO_2^-, SCN^- and F^- (Springer *et al.*, 1994), and many crystallographic studies have determined the structures of various globin molecules binding these anions (*e.g.* Conti *et al.*, 1993; Trent *et al.*, 2004; Yi *et al.*, 2008). However, an H-NMR study of *P. akamusi* Hb V reported for the first time that Cl^- can be an exogenous haem ligand to a globin protein (Yamamoto *et al.*, 2003) and the present study is the first crystallographic analysis to demonstrate the existence of haem-bound Cl^- in the globin molecule.

In our previous research (Kuwada *et al.*, 2010), we were unable to confirm the contribution of ArgE10 to stabilizing an exogenous ligand at acidic pH because the Arg side chain swings out towards the solvent region at acidic pH. Therefore, we considered the possibility that the water molecules present at the distal side of the haem, W2 and W3 shown in Fig. 1(*a*), act to stabilize the haem-bound ligand in aquomet Hb V at acidic pH, as is the case in bacterial Hb (Tarricone *et al.*, 1997). However, crystal structures of Hb V under high-salt conditions revealed the ArgE10 side chain on the distal haem face to form noncovalent bonds with the haem-bound Cl^- even at acidic pH (Figs. 1*b* and 3). Furthermore, preliminary MD simulations indicated that the behaviour of the Arg side chain was dependent on the difference in haem-bound ligand but not on the initial Arg conformation (Fig. 4). These results suggest that ArgE10 contributes to the characteristic Cl^- affinity as described by Yamamoto *et al.* (2003) and simultaneously that Cl^- binding to the haem iron can induce the

swinging movement of the Arg side chain into the haem pocket. We further considered the possibility that the water molecules on the distal side of the haem act as a kinetic barrier to prevent undesirable access of ligand molecules to the haem pocket, similar to those in deoxy Mb and *Mycobacterium* truncated Hb (Olson & Phillips, 1996; Ouellet *et al.*, 2007). However, Cl^- ligation at acidic pH predicted that these distal side water molecules have little or no effect against the Cl^- ion accessing Hb V under high salt concentration, in other words suggesting the presence of an attraction between the haem region and Cl^- ion that overcomes the barrier of the distal-side water molecules.

In contrast, no significant structural differences at the proximal side of the haem were observed between high-salt and salt-free conditions at acidic pH. Structural analyses of Hb V at different pH conditions indicated that pH change resulted in a coupled movement of ArgE10 and the C-terminal segment of the F helix with the haem movement (Kuwada *et al.*, 2010). Because a partial shift of the F-helix C-terminus towards the FG corner was observed at neutral pH concurrently with the swung-in conformation of ArgE10 and haem displacement, we considered the possibility that the stereochemical clash between the haem plane and the Arg side chain induces haem displacement towards the proximal side followed by a partial shift of the F helix (Kuwada *et al.*, 2010). The slight haem displacement towards the proximal side in Hb V under acidic and high-salt conditions (Fig. 3) also suggests that the side chain of ArgE10 on the distal haem face affects haem location. However, our present study indicates that the location of ArgE10 on the distal haem face has no significant effect on the stability of the F-helix C-terminus. Although this finding suggests that the partial shift of the F-helix C-terminus is an event that is independent of the ArgE10 movement, the mechanism that results in the F-helix movement in Hb V is unknown.

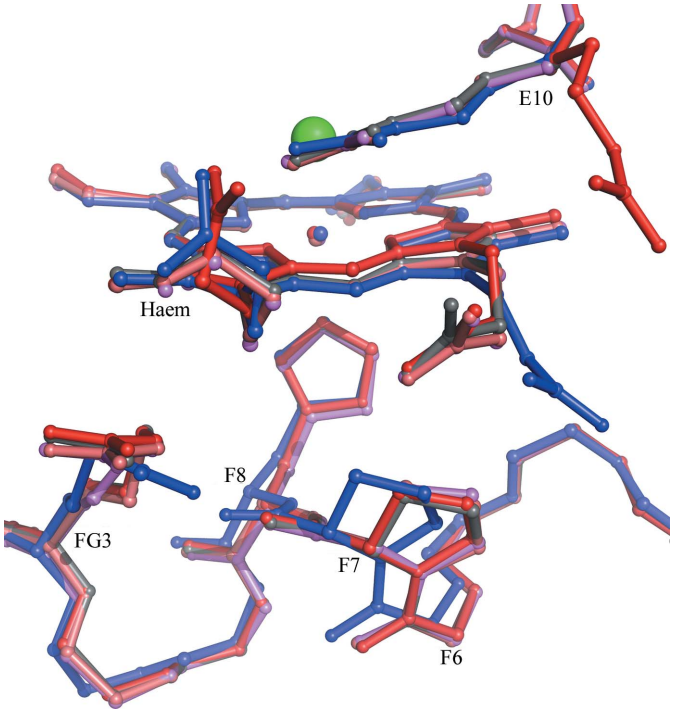

Figure 3
The haem region of Hb V at high salt concentration at acidic pH superposed on that at salt-free conditions at pH 4.6 (red) and pH 7.0 (blue; PDB entry 3a5g). The structures at 500 m*M* NaCl at pH 4.6, 1 *M* NaCl at pH 4.6 and 500 m*M* NaCl at pH 5.5 are shown in grey, salmon and violet, respectively. Except for the numbered residues ArgE10, GlyF6, ProF7, HisF8 and ArgFG3, the residues of the haem region are displayed as backbone atoms.

4.2. Predicted mechanisms of Cl^- binding and ArgE10 movement at acidic pH

The mechanisms that underlie the attraction that leads the Cl^- ion into the haem pocket at acidic pH and brings about the pH- and Cl^--binding-dependent swinging movement of ArgE10 are of particular interest. The pH-dependent change in electrostatic potential is one possible factor that affects the behaviour of ArgE10. Fig. 5 shows the electrostatic potential of the haem region of Hb V at acidic and neutral pH. This figure reveals the increased positive potential in the haem pocket at acidic pH compared with that at neutral pH. Although the electrostatic potential of the haem at each pH could not be calculated in the present study, Yamamoto *et al.* (2003) suggested that the haem propionate groups are protonated in Hb V at acidic pH. A simple suggestion derived from these findings is that the positively charged haem environment at acidic pH constrains the basic amino-acid Arg residue to swing out from the haem pocket. The electrostatic clash between the distal side of the haem and the Arg side

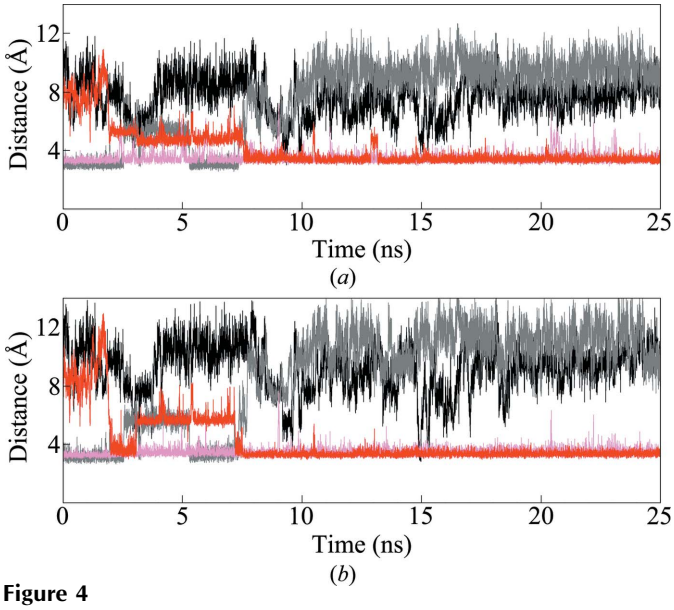

Figure 4
Time evolution of the distances between the haem ligand and (*a*) the N^{ε} atom and (*b*) NH of ArgE10. With two starting Hb V models, the ArgE10 swung-out form and the Arg swung-in form, we ran simulations for two different haem-bound ligands: a Cl^- ion and a water molecule. In the cases of Cl^- binding, results for the Arg swung-out and swung-in forms are shown in red and pink, respectively. In the cases of water binding, results for the Arg swung-out and swung-in forms are shown in black and grey, respectively.

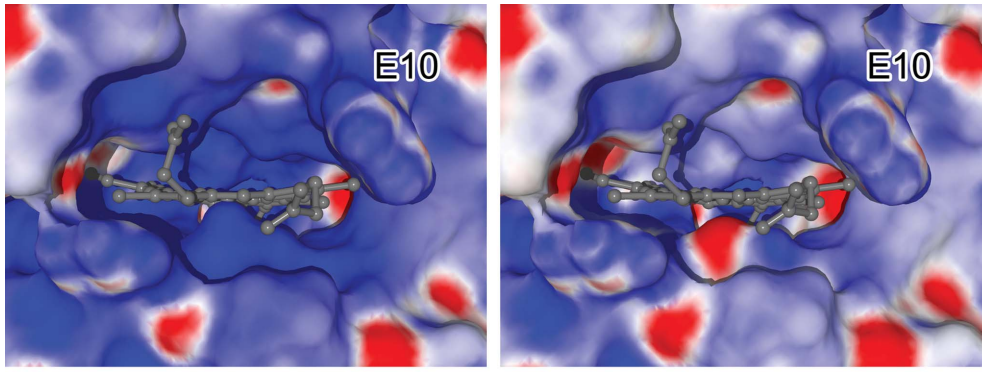

(*a*) (*b*)

Figure 5
Electrostatic surface of the Hb V haem pocket at pH 4.6 (*a*) and pH 7.0 (*b*). Red surfaces indicate negative potential and blue positive (±15 *kT*/e). The electrostatic surface at each pH was computed with the ArgE10 swung-out form for easy viewing of the haem pocket.

chain is likely to play an important role in tuning the acidic Bohr effect in Hb V. In contrast, the positively charged haem region can be expected to attract a Cl^- ion and lead to its binding. Binding of the Cl^- then decreases the electrostatic potential of the haem environment, resulting in the Arg side chain being able to swing into the haem pocket and remain on the distal haem face by forming noncovalent bonds with the Cl^- ion.

In addition to ArgE10 movement, we must also consider the suggestion by Yamamoto *et al.* (2003) that the stabilization of the haem-bound Cl^- requires a stronger hydrogen bond compared with that for haem-bound F^- in other globin proteins such as *A. limacina* Mb (Bolognesi *et al.*, 1990) because Cl^- possesses a weaker field strength than F^-. However, there is only one hydrogen bond between the Cl^- ion and ArgE10 at a distance of 3.2 Å in Hb V. Instead, because more Arg, Lys and Tyr residues are involved in the haem pocket of Hb V, the positive charge covers the haem region of Hb V extensively compared with that in *A. limacina* Mb, which can bind F^- to the haem iron (Supplementary Fig. 2). In Hb V at acidic pH, the increased and extended positive electrostatic potential in the haem environment may also contribute to stabilizing the haem-bound Cl^-.

Recent studies indicated that the electrostatic interaction between the haem-bound ligand and the distal polar residue in globin molecules plays an important role in ligand-binding properties such as ligand migration and the discrimination of differences in ligands (Springer *et al.*, 1994; Sigfridsson & Ryde, 2002). Interestingly, in *P. akamusi* Hb V changes in the overall electrostatic potential of the haem environment play a major role in anion binding *via* dynamic movement of the ArgE10 side chain. Conformational flexibility of the polar E10 residue and its contribution to ligand-binding properties have also been suggested in hexacoordinate globin proteins: ArgE10 in cytoglobin (Sugimoto *et al.*, 2004) and LysE10 in neuroglobin (Couture *et al.*, 2001; Fago *et al.*, 2004). It is probable that pH-dependent and ligation-dependent electrostatic changes in the haem region also occur in other globin molecules (Supplementary Fig. 2); therefore, observing the electrostatic potential might provide useful clues to understanding the behaviour of the distal polar residue in other globins at different pH conditions or in different ligand states.

This work was supported in part by Nihon University Multidisciplinary Research Grant (2009). We are grateful to Professor Hiroshi Iijima of the School of Pharmacy, Nihon University and Dr Yumiko Takahashi, Dr Keisuke Nakao and all the staff of LEBRA, Nihon University for their helpful technical advice.

References

Baker, N. A., Sept, D., Joseph, S., Holst, M. J. & McCammon, J. A. (2001). *Proc. Natl Acad. Sci. USA*, **98**, 10037–10041.
Baldwin, J. & Chothia, C. (1979). *J. Mol. Biol.* **129**, 175–220.
Bas, D. C., Rogers, D. M. & Jensen, J. H. (2008). *Proteins*, **73**, 765–783.
Bolognesi, M., Coda, A., Frigerio, F., Gatti, G., Ascenzi, P. & Brunori, M. (1990). *J. Mol. Biol.* **213**, 621–625.
Chen, V. B., Arendall, W. B., Headd, J. J., Keedy, D. A., Immormino, R. M., Kapral, G. J., Murray, L. W., Richardson, J. S. & Richardson, D. C. (2010). *Acta Cryst.* D**66**, 12–21.
Collaborative Computational Project, Number 4 (1994). *Acta Cryst.* D**50**, 760–763.
Conti, E., Moser, C., Rizzi, M., Mattevi, A., Lionetti, C., Coda, A., Ascenzi, P., Brunori, M. & Bolognesi, M. (1993). *J. Mol. Biol.* **233**, 498–508.
Couture, M., Burmester, T., Hankeln, T. & Rousseau, D. L. (2001). *J. Biol. Chem.* **276**, 36377–36382.
DeLano, W. L. (2002). *PyMOL.* http://www.pymol.org.
Dolinsky, T. J., Nielsen, J. E., McCammon, J. A. & Baker, N. A. (2004). *Nucleic Acids Res.* **32**, W665–W667.
Fago, A., Hundahl, C., Dewilde, S., Gilany, K., Moens, L. & Weber, R. E. (2004). *J. Biol. Chem.* **279**, 44417–44426.
Fukuda, M., Takagi, T. & Shikama, K. (1993). *Biochim. Biophys. Acta*, **1157**, 185–191.
Golovin, A. & Henrick, K. (2008). *BMC Bioinformatics*, **9**, 312.
Guex, N. & Peitsch, M. C. (1997). *Electrophoresis*, **18**, 2714–2723.
Hess, B., Kutzner, C., van der Spoel, D. & Lindahl, E. (2008). *J. Chem. Theory Comput.* **4**, 435–447.
Kamimura, S., Matsuoka, A., Imai, K. & Shikama, K. (2003). *Eur. J. Biochem.* **270**, 1424–1433.
Koshikawa, K., Yamamoto, Y., Kamimura, S., Matsuoka, A. & Shikama, K. (1998). *Biochim. Biophys. Acta*, **1385**, 89–100.
Kuwada, T., Hasegawa, T., Sato, S., Sato, I., Ishikawa, K., Takagi, T. & Shishikura, F. (2007). *Gene*, **398**, 29–34.
Kuwada, T., Hasegawa, T., Takagi, T., Sato, I. & Shishikura, F. (2010). *Acta Cryst.* D**66**, 258–267.

Li, H., Robertson, A. D. & Jensen, J. H. (2005). *Proteins*, **61**, 704–721.
Mattevi, A., Gatti, G., Coda, A., Rizzi, M., Ascenzi, P., Brunori, M. & Bolognesi, M. (1991). *J. Mol. Recognit.* **4**, 1–6.
Numoto, N., Nakagawa, T., Kita, A., Sasayama, Y., Fukumori, Y. & Miki, K. (2008). *Biochemistry*, **47**, 11231–11238.
Olson, J. S., Mathews, A. J., Rohlfs, R. J., Springer, B. A., Egeberg, K. D., Sligar, S. G., Tame, J., Renaud, J. P. & Nagai, K. (1988). *Nature (London)*, **336**, 265–266.
Olson, J. S. & Phillips, G. N. (1996). *J. Biol. Chem.* **271**, 17593–17596.
Oostenbrink, C., Villa, A., Mark, A. E. & van Gunsteren, W. F. (2004). *J. Comput. Chem.* **25**, 1656–1676.
Ouellet, H., Milani, M., LaBarre, M., Bolognesi, M., Couture, M. & Guertin, M. (2007). *Biochemistry*, **46**, 11440–11450.
Phillips, S. E. (1980). *J. Mol. Biol.* **142**, 531–554.
Phillips, S. E. & Schoenborn, B. P. (1981). *Nature (London)*, **292**, 81–82.
Shaanan, B. (1983). *J. Mol. Biol.* **171**, 31–59.
Sigfridsson, E. & Ryde, U. (2002). *J. Inorg. Biochem.* **91**, 101–115.
Springer, B. A., Sligar, S. G., Olson, J. S. & Phillips, G. N. Jr (1994). *Chem. Rev.* **94**, 699–714.
Sugimoto, H., Makino, M., Sawai, H., Kawada, N., Yoshizato, K. & Shiro, Y. (2004). *J. Mol. Biol.* **339**, 873–885.
Tarricone, C., Galizzi, A., Coda, A., Ascenzi, P. & Bolognesi, M. (1997). *Structure*, **5**, 497–507.
Trent, J. T. III, Kundu, S., Hoy, J. A. & Hargrove, M. S. (2004). *J. Mol. Biol.* **341**, 1097–1108.
Winn, M. D., Isupov, M. N. & Murshudov, G. N. (2001). *Acta Cryst.* D**57**, 122–133.
Xiao, Y., Wang, H., George, S. J., Smith, M. C., Adams, M. W., Jenney, F. E., Sturhahn, W., Alp, E. E., Zhao, J., Yoda, Y., Dey, A., Solomon, E. I. & Cramer, S. P. (2005). *J. Am. Chem. Soc.* **127**, 14596–14606.
Yamamoto, Y., Koshikawa, K., Terui, N., Mita, H., Matsuoka, A. & Shikama, K. (2003). *Biochim. Biophys. Acta*, **1652**, 136–143.
Yi, J., Safo, M. K. & Richter-Addo, G. B. (2008). *Biochemistry*, **47**, 8247–8249.